RESEARCH ARTICLE
Cytoskeleton, April 2015 72:182–192 (doi: 10.1002/cm.21218)

Effects of the Dynein Inhibitor Ciliobrevin on the Flagellar Motility of Sea Urchin Spermatozoa

Yuuko Wada,[1]* Shoji A. Baba,[2] and Shinji Kamimura[1]

[1]*Department of Biological Sciences, Faculty of Science and Engineering, Chuo University, Tokyo, Japan*
[2]*Department of Biology, Ochanomizu University, Tokyo, Japan*

Received 6 October 2014; Revised 6 March 2015; Accepted 18 March 2015
Monitoring Editor: Ritsu Kamiya

Ciliobrevin has recently been found to be a membrane-permeable inhibitor that is specific to AAA+ molecular motors such as cytoplasmic dyneins. In this study, we investigated how ciliobrevin inhibited the motility of sperm from sea urchins: *Hemicentrotus pulcherrimus*, *Pseudocentrotus depressus*, and *Anthocidaris crassispina*. After application of 100 μM of ciliobrevin A to live spermatozoa, swimming speed decreased gradually and flagellar motion stopped almost completely within 5 to 10 min. This inhibition was reversible and the frequency of flagellar beating was reduced in a concentration-dependent manner. Ciliobrevin had similar inhibitory effects on the flagellar beating of demembranated and reactivated sperm and the sliding disintegration of trypsin-treated axonemes. We also analyzed the curvature and shear angle of the beating flagella and found that the proximal region of the sperm flagellum was less sensitive to ciliobrevin compared with more distal regions, where bending motions were blocked completely. Interestingly, the shear angle analysis of flagellar motility showed that ciliobrevin induced highly asymmetric bends in the proximal region of the flagellum. These results suggest that there is heterogeneity in the inhibitory thresholds of dynein motors, which depend on the regions along the flagellar shaft (proximal or distal) and on the sites of doublets in the flagellar cross-section (doublet numbers). We expect that it will be possible to map the functional differences in dynein subtypes along and/or around the cross-sections of flagellar axonemes by analyzing the inhibitory effects of ciliobrevin. © 2015 Wiley Periodicals, Inc.

Additional Supporting Information may be found in the online version of this article.

*Address correspondence to: Yuuko Wada, Department of Biological Sciences, Faculty of Science and Engineering, Chuo University, Kasuga 1-13-27, Tokyo 112-8551, Japan.
E-mail: ywada@bio.chuo-u.ac.jp

Published online 25 March 2015 in Wiley Online Library (wileyonlinelibrary.com).

Key Words: heterogeneity of dyneins; AAA+molecular motors; beat frequency; asymmetry index; amputated flagella

Introduction

Ciliobrevin is a specific and membrane-permeable inhibitor of AAA+ ATPases (ATPases associated with diverse cellular activities) such as cytoplasmic dyneins [Firestone et al., 2012]. It has been shown to reduce the length of primary cilia, to disrupt the polar microtubule assembly of mitotic spindles, to inhibit melanosome aggregation and peroxisome motility, and to reduce the rate of intracellular transportation and microtubule sliding on cytoplasmic dynein (in vitro motility assay) in a concentration-dependent manner. It was also shown that ciliobrevin inhibits intraflagellar transport and gliding motility, which is powered by cytoplasmic dynein1b in *Chlamydomonas* [Shih et al., 2013].

Axonemal dyneins, which are also classified as members of the AAA+ superfamily [Mocz and Gibbons, 2001; reviewed in King, 2012], are major motor components of eukaryotic cilia and flagella. Depending on their sites on doublet microtubules in the cross-sections of axonemes, axonemal dyneins are grouped into two major types: the outer and inner dynein arms, both of which hydrolyze ATP and contribute to beating of cilia or flagella. The outer dynein arms, which comprise two or three dynein heavy chains, appear to operate as force generators and they are crucial for determining the rate of flagellar beating. The inner dynein arms, which comprise several different types of single- or two-headed isomers, are responsible for regulating the flagellar beat patterns in *Chlamydomonas reinhardtii* [Brokaw and Kamiya, 1987].

Sea urchin spermatozoa have been proved useful for the detailed analysis of flagellar waveforms and their regulatory mechanisms in the study of flagellar/ciliary motility. Unlike mammalian sperm, sea urchin sperm flagella have simple 9 + 2 axonemes without a stiff mid-piece encircled with a

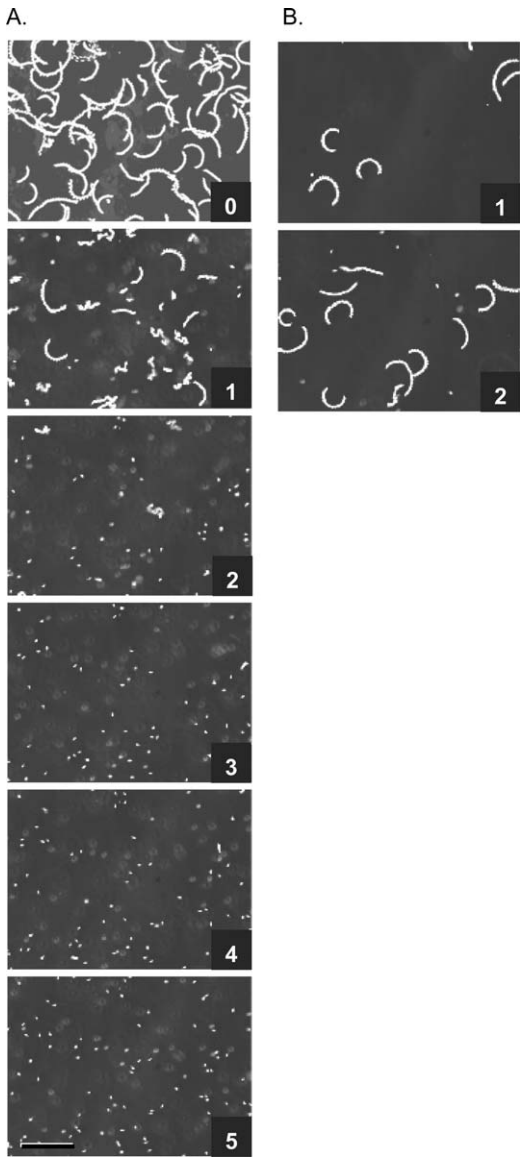

Fig. 1. Ciliobrevin inhibited the motility of sea urchin sperm in a reversible manner The swimming paths of sea urchin sperm (*Anthocidaris crassispina*) after applying 100 μM ciliobrevin were obtained by superimposing 100 successive frames from high-speed video image recordings (200 fps). The numbers indicate the time (min) after applying and washing ciliobrevin (100 μM) in (**A**) and (**B**), respectively. Swimming was inhibited almost completely by ciliobrevin within 5 min but it was restored after removal. Scale bar, 50 μm.

mitochondrial sheath, or accessory outer dense fibers. Thus, we can expect that the shear angle rate or the beat frequency directly represents the active interactions between axonemal dyneins and the outer doublet microtubules. In addition, their flagellar beating are highly planar allowing us to analyze the detailed waveforms in various experimental conditions. Thus, sea urchin sperm flagella may provide a suitable assay system for investigating the effects of dynein inhibitors in detail.

In the present study, we investigated how ciliobrevin functions as a potent inhibitor of axonemal dyneins; and we examined its inhibitory effects on the waveform parameters related to flagellar motility in sea urchin spermatozoa. In particular, we focused on the difference in the inhibition

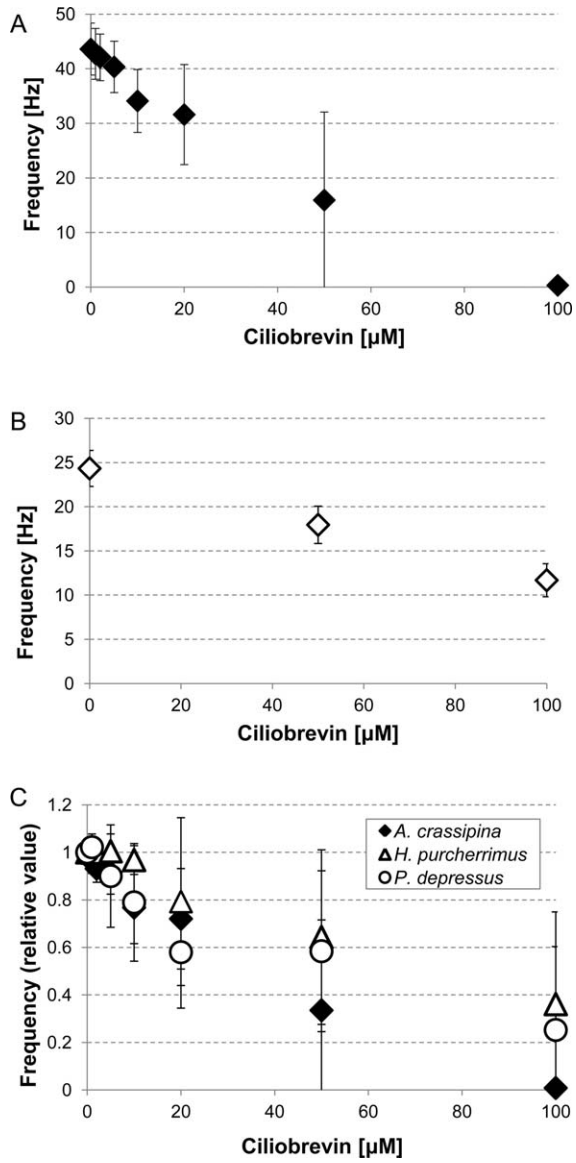

Fig. 2. Ciliobrevin reduced the flagellar beat frequency in a concentration-dependent manner. (**A**) Series showing the concentration-dependent effects of ciliobrevin inhibition on the sperm beat frequency of *A. crassispina*. Each data point (mean ± SD) was obtained based on about 600 spermatozoa in 20 independent experiments to determine the beat frequency in observations under stroboscopic dark-field illumination. (**B**) Inhibition of the motility of demembranated spermatozoa by ciliobrevin. Data from three independent experiments are shown. The inhibitory effects remained after removing the flagellar membrane. (**C**) Summary of the concentration-dependent effects in all of the sea urchin species tested. The relative beat frequencies normalized against the control values are shown, i.e., 43.6, 33.5, and 32.8 Hz for *A. crassispina* (20 independent experiments), *P. depressus* (four experiments), and *H. pulcherrimus* (eight experiments), respectively. There were differences in sensitivity that depended on the sea urchin species, but the inhibition appeared consistently in a concentration-dependent manner.

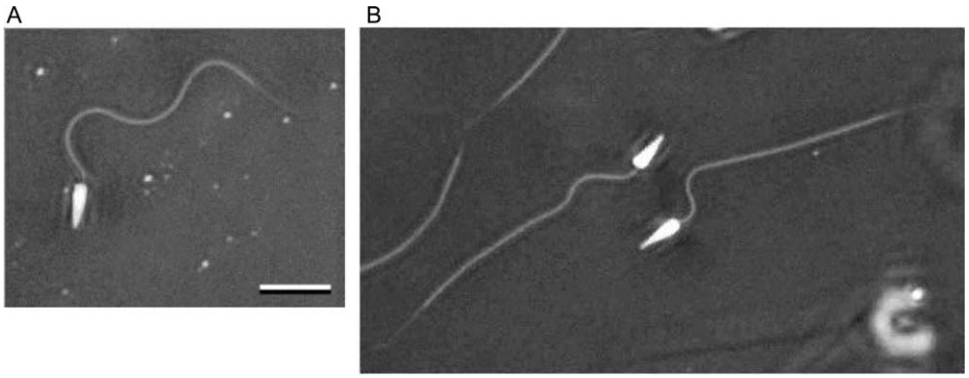

Fig. 3. Effect of ciliobrevin on the flagellar beat waveforms. High-speed video image recordings of *A. crassispina* spermatozoa beating in control conditions (**A**), and in the presence of 100 μM ciliobrevin (**B**). In the presence of 100 μM ciliobrevin, many spermatozoa stopped swimming or they beat with a very low frequency (<1 Hz) as shown in (B). This slow beating continued for a couple of minutes and the motion ceased as the frequency decreased. In general, the propagation of beating waves was restricted only to the proximal regions of the flagella, as shown in the figure. Scale, 10 μm.

thresholds for beat rates and bend angles to determine how ciliobrevin functions differently in various types of axonemal dyneins, i.e., how the inhibitory effect depends on the dynein motor functions in the outer and inner dynein arms, or on hypothetical localizations along the flagellar shaft.

Results

Ciliobrevin Reversibly Inhibits the Flagellar Motility of Sea Urchin Sperm

In control conditions, using an artificial seawater medium containing bovine serum albumin (BSA-ASW), sea urchin (*Anthocidaris crassispina*) spermatozoa swam in circles near the surfaces of the cover slips, as described previously [Gibbon and Gibbons, 1972; Hiramoto and Baba, 1978]. The mean beat frequency and swimming velocity were, 30–40 Hz and approximately 100 μm/s, respectively. However, after application of 100 μM ciliobrevin A (HPI-4), swimming speed of spermatozoa decreased gradually and almost all of the observed spermatozoa stopped swimming within 5 min (Fig. 1, movie S1 in Supporting Information). When the ciliobrevin was washed away by perfusing with fresh BSA-ASW in the experimental chamber, the inhibitory effects were found to be partially reversible. Within 2 min, around 40% of the spermatozoa exhibited restored swimming activities, which were almost at the control level in terms of speed and beat frequency (Fig. 1, movie S1 in Supporting Information). Some of the remaining immotile spermatozoa were observed to be adhered to the glass surfaces, or they were immotile for other unknown reasons.

Inhibitory Effect of Ciliobrevin on the Beat Frequency

Because we found that 100 μM ciliobrevin had strong inhibitory effects in stopping sperm motility, we investigated its concentration dependency in more detail. Figure 2A shows that the beat frequency of *A. crassipina* sperm flagella was reduced in a concentration-dependent manner.

The hydrophobic ciliobrevin molecule is assumed to be membrane permeable, but it could function indirectly by affecting membrane proteins, rather than affecting the activity of axonemal dyneins directly. To exclude this possibility, we also tested its effects on Triton-demembranated spermatozoa. In the case of *A. crassipina* spermatozoa, the effects appeared to be slightly weaker than those on live spermatozoa, although we observed similar inhibitory effects (Fig. 2B), i.e., ciliobrevin decreased the beat frequency by about 50% at 100 μM. We also found that there was a small difference in the inhibitory effects, which depended on the sea urchin species we used in the present study. Slightly greater inhibitory effects were observed in *A. crassispina* spermatozoa compared with those in the other species, *Pseudocentrotus depressus* and *Hemicentrotus pulcherrimus* (Fig. 2C).

Effects of Ciliobrevin on the Beat Waveform of Sperm Flagella

We found that ciliobrevin inhibits flagellar motility, which is based on different dynein species, axonemal dyneins. A typical effect of inhibition was a decrease in the frequency of flagellar beating, but we often observed that the sperms showed some characteristic changes in their beat forms, i.e., the distal tail regions were completely immotile in a straight form, whereas the proximal regions of the flagella continued to beat but with no wave propagations (Figs. 3 and 4A, movie S3 in Supporting Information). Similar inhibition of the propagation of bending waves was observed in the reactivated axonemes after Triton demembranation. At the same time, the bend formed at the base of the flagella was obviously different and asymmetric compared with the regular waveforms generated in the control spermatozoa.

These features were clear when we performed a detailed analysis of the wave parameters. Figures 4B and 4C show

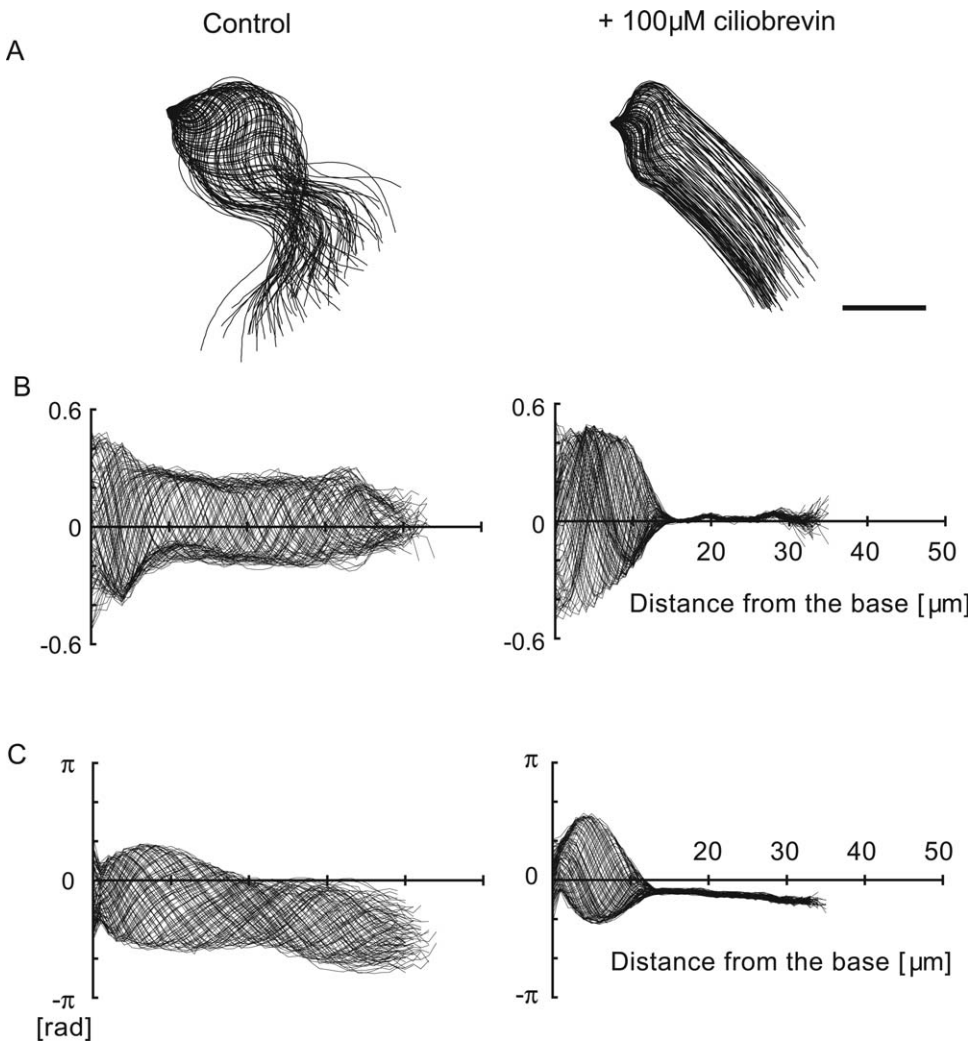

Fig. 4. Comparisons of flagellar waveform parameters. (**A**) Flagellar waveforms of a typical control spermatozoon (left), and that in the presence of 100 μM ciliobrevin (right). Superimposed traces of flagellar forms from 500 ms recordings are shown, where the positions of the sperm heads are fixed. Scale bar, 10 μm. (**B**) Superimposed data showing the bending curvatures and the inverse of the curvature radii, which were obtained from the *XY*-coordinates of sperm tails from 100-frame video series and plotted against the distance from the proximal end of the flagellum. In the control spermatozoa, bends with high curvatures propagated well along the flagellum to the distal end. After inhibition with 100 μM ciliobrevin, new bends (with slightly higher curvatures compared with control flagella) degraded rapidly at around 15 μm from the proximal end. (**C**) Shear angle data. In the control spermatozoa, the shear angle varied in a regular manner, thereby indicating continuous wave propagation. Ciliobrevin did not block bending around the proximal region of flagella, but it stopped wave propagation to the distal end completely.

the superimposed curvature and shear angle data, obtained from 100 frames (duration of 0.5 s), respectively. In a typical case of control flagellar beating (Fig. 4, left column; movie S2 in Supporting Information), the bends generated at the proximal base region propagated along the flagellum without any decline in bend curvature. In the presence of 100 μM of ciliobrevin (Fig. 4, right column; movie S3 in Supporting Information), new bends with similar curvatures were generated at the base end. However, they decayed rapidly when they progressed further than 10 μm from the base end of the flagellum. Based on 21 different records of flagellar motions (100 frames each) that exhibited rapid declines in their curvatures in the presence of 100 μM of ciliobrevin, we tentatively determined the mean active length of the flagella as 12.9 ± 1.6 μm (Fig. 5). According to these estimates, we suggest that there is a narrow border zone on the flagellar shaft beyond which the inhibitory effects of dynein activity by ciliobrevin appear abruptly.

Effect of Ciliobrevin on the Motility of Short Flagella

Since the inhibitory effects differed between the proximal and distal parts of sperm flagella (Figs. 3 and 4), we investigated how these effects appeared in the proximal region alone if there were no distal parts, i.e., in short amputated flagella that only possessed the proximal parts of the

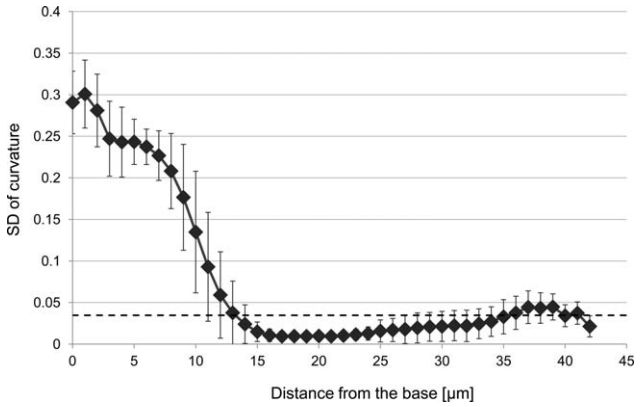

Fig. 5. Flagellar bends were restricted only to the proximal regions of axonemes in the presence of ciliobrevin. In order to determine the magnitudes of the periodic curvature changes, we calculated the standard deviations of the curvature curves obtained during 100 successive video frames in 21 experiments. The broken horizontal line represents the average deviation value for the curvature calculated in the distal 10 μm nonmotile regions. Based on the crossing point of the deviation curve and the horizontal line, we determined the length limit for wave propagation. In the case of *A. crassispina*, as shown here, the limit was 12.9 ± 1.6 μm from the proximal end.

flagella. After passing sperm specimens through a fine needle, we obtained spermatozoa with various flagella lengths. Figure 6 shows superimposed images of five video frames with beating flagella in the presence of 100 μM ciliobrevin (the original video recording is also provided as movie S4 in the Supporting Information), which is the concentration at which the distal parts of flagella stopped beating (Fig. 2A). In many cases, these short flagella remained motile for more than 30 min. Therefore, it is clear that the threshold of ciliobrevin inhibition differs between the proximal and distal parts, depending on the site along the flagella. We found that the beat waveforms of these short flagella were highly asymmetric and they closely resembled the beat patterns of cilia (Fig. 7A); hence, we then compared these wave parameters.

Ciliobrevin Changed the Beat Waveforms of Flagella into a Cilium-Like Asymmetric Pattern

In general, flagellar and ciliary beating can be distinguished by comparing the time course of shear angle variations in the proximal base regions of axonemes. In ciliary motions, there is a large difference in the phase velocity between beats, i.e., fast effective and slow reverse stroke phases. The difference in the shear angle rate is obvious, as shown in an example of ciliary beats observed in sea urchin embryos in Fig. 7C [Wada et al., 1997]. Although the severed short flagella of sea urchin spermatozoa appeared to beat like cilia, the pattern of the beats was rather symmetric compared with the ciliary beating. To depict the magnitude of asymmetry in a more direct manner, we obtained plots of the shear angles of long (intact) and short (amputated) flagella, which were observed with or without ciliobrevin (Fig. 7B). We compared these with those obtained using cilia from sea urchin embryos (Fig. 7C). Intact (full length) sperm without ciliobrevin exhibited almost symmetrical variations in their shear angle changes in the proximal region (5 μm from the base). The velocities of the angle changes toward the principal and reverse bend directions were almost the same, as shown in Fig. 7B. This was also the case for severed flagella (length, 10–15 μm). By contrast, the shear angle profile of flagellar beating in the presence of 100 μM ciliobrevin was asymmetric in both the full-length and amputated flagella, as observed in cilia (Figs. 7B and 7C). The observed rate of the fast phase resembled that in the ciliary effective strokes of cilia. In some cases, we confirmed that the fast phases corresponded to the direction of the principal bends, which were usually located outside the circle of the swimming path of spermatozoa. In other cases, particularly the amputated flagella, we could not determine the direction of the principal bends, but we assumed that the observed fast phase corresponded to the side of the principal bends.

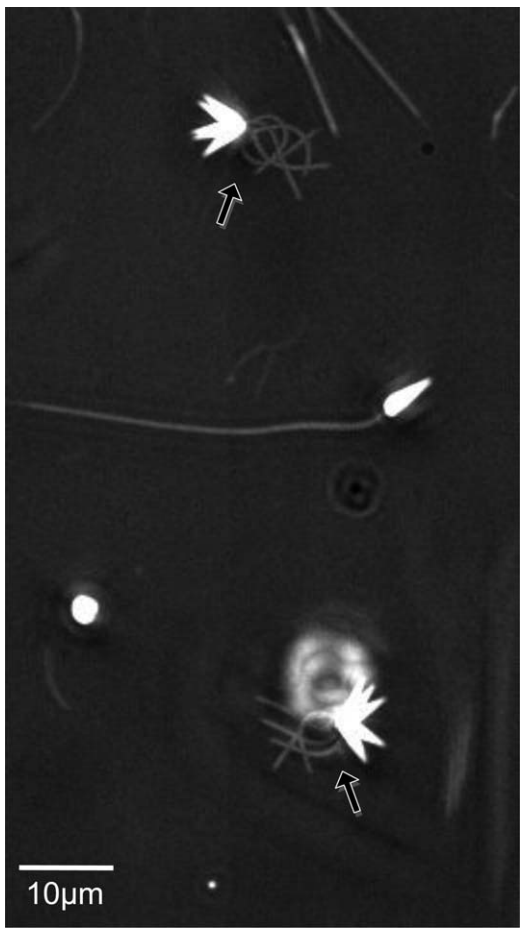

Fig. 6. Short flagella beat like cilia in the presence of ciliobrevin. Five superimposed images from video recording, which show the motions of amputated sea urchin sperm flagella. Spermatozoa with various lengths of flagella were obtained by pipetting and 100 μM ciliobrevin was applied. Scale, 10 μm.

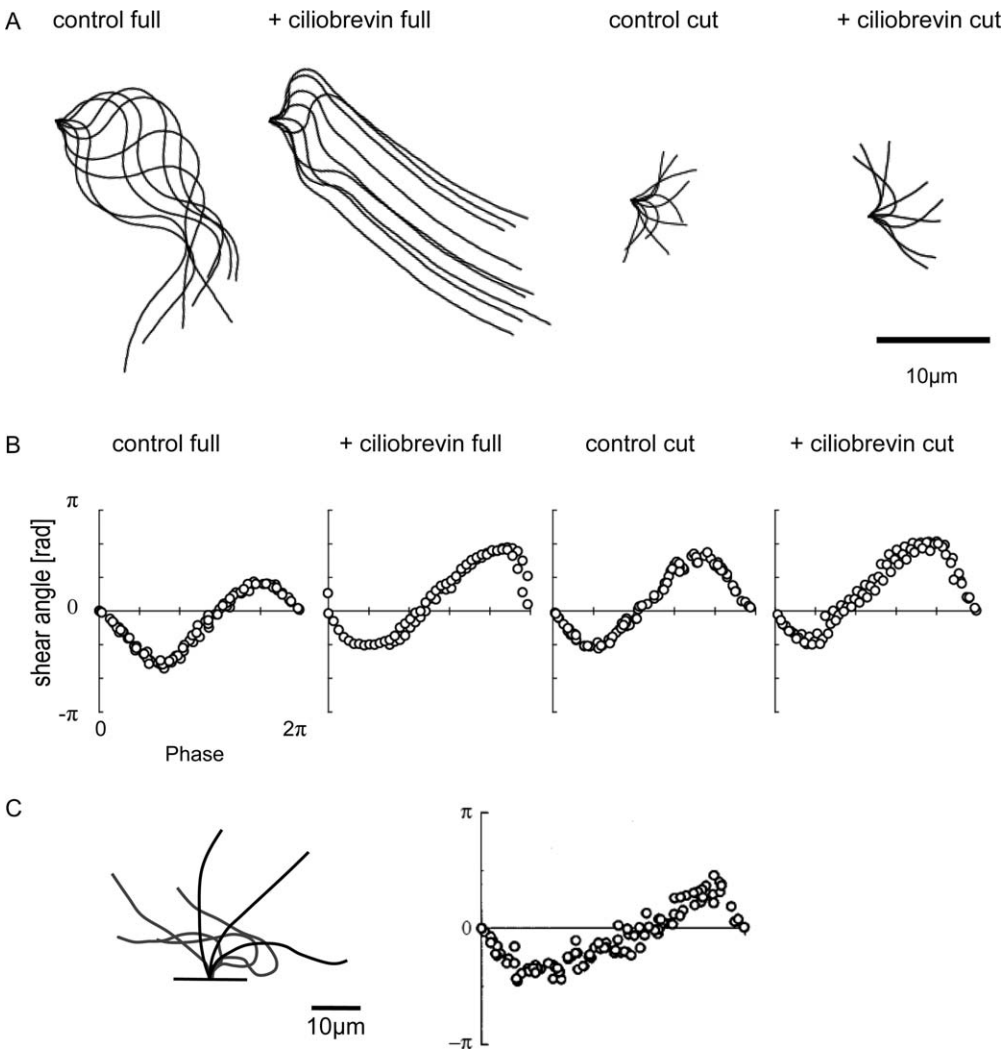

Fig. 7. Beating characteristics of short flagella. (**A**) Superimposed traces from video recordings. From the left, waveforms of full length spermatozoa (control and with ciliobrevin) and severed sperm flagella (control and with ciliobrevin) are shown. (**B**) To compare the beat asymmetry, the superimposed shear angle changes at the site 5 μm from the flagellar base during one beat cycles are shown, after normalizing the amplitude ($\pm\pi$) and phase (0 to 2π) scales. (**C**) Example of a ciliary beat. Both the superimposed waveforms and the shear angle analysis results are shown. The data for cilia are modified from figures in Wada et al. [1997].

The time course of shear angular changes at a given point along sperm axonemes is known to be sinusoidal [Hiramoto and Baba, 1978]. This indicates that the active sliding in the peripheral microtubules can be described as a sinusoidal function of time, $A_0 \cdot \sin(\omega t + \delta)$. Thus, we tried to fit sinusoidal functions to the shear angle curves obtained at the point located 5 μm distant from the flagellar base. However, this fitting was not successful in the cases where sperm flagella were inhibited by ciliobrevin and in embryonic cilia. In order to illustrate the magnitude of the beating asymmetry, we used a new parameter: the asymmetry index. First, we fitted the bend angle curve to a composite asymmetric curve formed of two sine waves with different phase velocities: ω_{up} and ω_{down}, i.e., $A_0 \cdot \sin(\omega_{up} \cdot t + \delta_{up})$ for the ascending phase and $A_0 \cdot \sin(\omega_{down} \cdot t + \delta_{down})$ for the descending phase (Fig. 8 inset). δ_{up} and δ_{down} are constants used to compensate for phase differences. The new asymmetry index was then defined by calculating the ratio of the two phase velocities: $\omega_{down}/\omega_{up}$, which represents the relative ratio of the wavelength for the two sine curves, or the ratio of the time period required for beating in the faster ascending (principal bend) and slower descending (reverse bend) phases, respectively.

In the control conditions without ciliobrevin, both the full- and short-length flagella had similar asymmetry indices of 1.0 ± 0.02 ($n = 10$), which indicated that their motions were almost symmetric ($\omega_{up} \sim \omega_{down}$). This also means that pure sine curves can be fitted well to the time course profile of the shear angle without any modifications. However, this value became larger in the presence of ciliobrevin, and in some cases it exceeded 5, i.e., the descending phase was more than five times longer compared with the ascending phase. Thus, it is obvious that ciliobrevin converted the symmetric beats of sea-urchin sperm flagella into highly

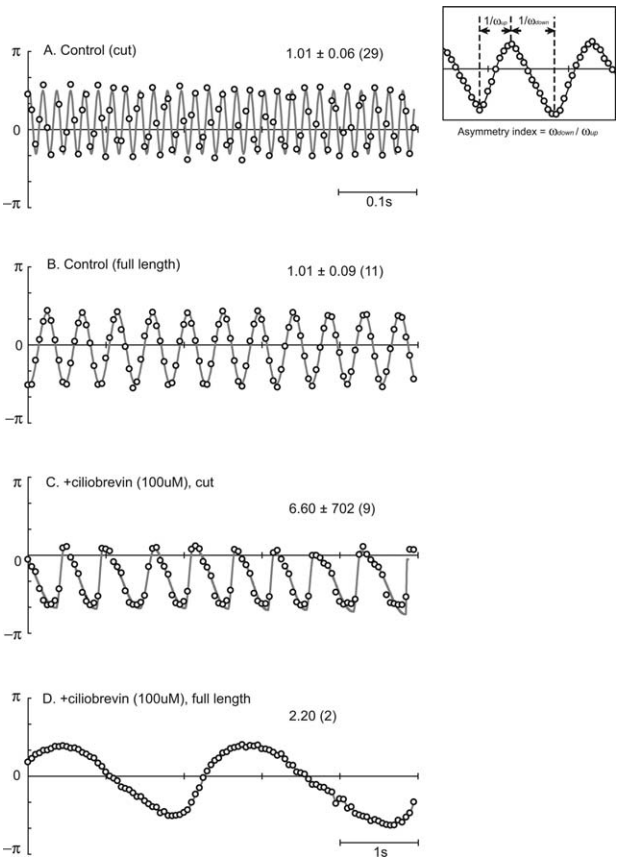

Fig. 8. Quantitative analysis of beat asymmetry. Time course variations in the shear angles at the point located 5 μm from the flagellar base. (**A**) and (**B**) Data from control short and full-length flagella, respectively. (**C**) and (**D**) Data from short and full-length flagella in the presence of 100 μM ciliobrevin, respectively. We calculated the asymmetry indices by fitting biased sine waves: $A_0 \cdot \sin(\omega_{up} \cdot t + \delta_{up})$ and $A_0 \cdot \sin(\omega_{down} \cdot t + \delta_{down})$, for the ascending and descending phases, respectively. Based on the fitted curves, an asymmetry index was defined: $\omega_{udown}/\omega_{up}$ (inset figure). The index should be 1.0 for symmetric beating with equal rates in the ascending and descending phases. Each number on the right indicates the mean value of the asymmetry index ± S.D. (number of waves). Note that the shorter flagella beat faster in both the control and ciliobrevin-inhibited conditions. The time scale is 10 times longer in (D). In the control conditions, the value of the asymmetry index was close to 1 with small periodic variations. In the presence of ciliobrevin, the values were high and variable, thereby indicating that the beating was asymmetric and unstable. In (D), the standard deviation could not be calculated because the recorded beating was less than three beat cycles.

asymmetric forms similar to ciliary beats. These features were evident in the proximal regions of axonemes, where the motile activity was retained even in the presence of 100 μM ciliobrevin.

Effect of Ciliobrevin on the Sliding Disintegration of Axonemes

To see the inhibitory effects of ciliobrevin on dyneins more directly, we performed sliding disintegration experiments. As shown in Fig. 9, we found that ciliobrevin also inhibited the microtubule sliding. In the case of axonemes treated with ciliobrevin for more than 5 min, sliding disintegration was significantly inhibited (Fig. 9A). Interestingly, in some axonemes which appeared to be intact showed partial and slow (1–2 Hz) bending. In the case of ciliobrevin treating for more than 10 min, there were neither trypsin-induced disintegration nor slow bending. In the case of ciliobrevin treating for less than 5 min, the measured velocity of microtubule sliding in disintegrating axonemes was reduced (Fig. 9B) though disintegration percentage was as high as the control.

Discussion

Inhibitory Effects of Ciliobrevin on the Motility of Sea Urchin Sperm Flagella

Based on the present study, it is obvious that ciliobrevin inhibits the motility of sea urchin sperm flagella. It reduced the flagellar beat frequency and almost stopped motility within 5 min at 100 μM in the case of *A. crassipina*. These inhibitory effects were reversible (Fig. 1B) and they occurred in a concentration-dependent manner (Fig. 2A). The waveform of the flagellar beating also varied (Figs. 2 and 3), which may indicate that ciliobrevin affects both the outer arm (related to motion speed) and inner arm (waveform regulators) dyneins. Inhibition was also observed in a demembranated sperm model (Fig. 2B) and in the sliding disintegration of axonemes (Fig. 9), thus the inhibitory effects influenced the axonemal dynein ATPases directly.

In live spermatozoa (Fig. 2A), the standard deviation of the beat frequency was high, especially at around 50 μM, because some spermatozoa stopped and others continued swimming at almost the same frequency as the control spermatozoa with no ciliobrevin. This suggests that the threshold for inhibition may vary among individual spermatozoa. The standard deviation of the beat frequency in demembranated spermatozoa was relatively small (Fig. 2B), so the effects on the live sperm population would have varied due to differences in ciliobrevin membrane permeability, or due to other soluble intracellular factors.

Nonuniformity of the Sites Affected by Ciliobrevin

The inhibitory effects of ciliobrevin did not appear to be uniform along the lengths of axonemes and the threshold for inhibition differed between the proximal and distal regions of flagella (Figs. 3–5), as well as between the principal and reverse bends (Figs. 6–8). The proximal regions of axonemes appeared to have a higher threshold and they continued to move even in the presence of 50 to 100 μM ciliobrevin, whereas the distal regions (>13 μm from the base) stopped moving completely (Fig. 5). The observed bend shapes in the proximal region with inhibition were

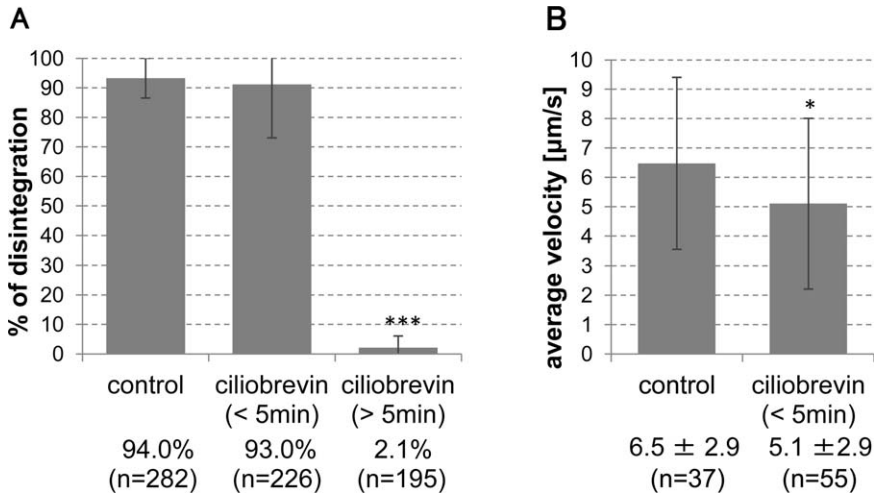

Fig. 9. Sliding disintegration experiments. (**A**) Percentage of disintegrated axonemes. The disintegration percentage was significantly reduced after the incubation with ciliobrevin more than 5 min ($P < 0.005$). (**B**) Comparison of sliding velocities measured in control and in treated axonemes ($P < 0.05$).

almost the same as those in the curved area in Ca^{2+}-quiescent spermatozoa [Gibbons, 1980]. This suggests that some of the dynein activities related to Ca^{2+}-insensitive sliding in the proximal region may be insensitive to ciliobrevin. Interestingly, the length of the ciliobrevin-insensitive area (~13 μm from the base) almost corresponded to that of the flagellar severed by pipetting [Baba, unpublished data]. Thus, these dynein properties might be correlated with the mechanical robustness of axonemes. The evidence obtained in the present study suggests that there is a border in the axonemal area where the dyneins have different structural and/or functional properties at around 13 μm distant from the flagellar base. Presumably, there is a difference in the affinity of ciliobrevin for the dynein ATPases in these two regions, which would explain the differences in the dynein properties. We expect that the difference in the threshold of inhibition is due to variations in the dynein species and the structure of their ATP-binding sites, i.e., variations in the roles and functions of dynein along axonemes.

We also observed asymmetric beating in sperm flagella that resembled ciliary motions, particularly in short amputated flagella (Fig. 6) after inhibition by ciliobrevin. The shear angle profiles at the proximal regions (5 μm from the base) in both long intact and short severed sea urchin sperm flagella were quite similar (Fig. 7). In the long flagella, we initially assumed that the long immotile tails inhibited by ciliobrevin provided mechanical obstruction against normal microtubule sliding, thereby generating specific asymmetric waves in the proximal region. However, our detailed analysis of the shear angle variations in the proximal regions showed clearly that, the effects of ciliobrevin were not due simply to mechanical resistance, but instead they induced asymmetry in the flagellar beating.

After comparing the time courses between the ascending and descending phases of the shear angle curves, we defined a parameter to indicate the magnitude of asymmetry (Figs. 7B and 7C). The observed fast and slow phases corresponded to the effective and recovery strokes, respectively, in the case of ciliary beats. It is known that flagellar beating comprises two bends in opposite directions: principal and reverse bends. In control conditions, the angle amplitude of the principal bends is usually larger than that of the reverse bends, which generates the circular paths of sperms that swim with principal bends outside the circles. Similarly, even in the short amputated flagella, there were differences in amplitude between the fast and slow phases (Fig. 7B), which corresponded to the principal and reverse bends, respectively. Thus, we can assume that a specific regulatory mechanism operates to maintain the "amplitude asymmetry" or "rate asymmetry" during axonemal bending in the control flagella, when not inhibited by ciliobrevin. We showed that both bends had a similar angular phase velocity ($\omega_{up} \sim \omega_{down}$), thus we also suggest that the motion phase was almost symmetric, i.e., a mechanism with "phase symmetry." The results of this study indicate clearly that ciliobrevin primarily inhibits the formation of reverse bends. This suggests that there is a difference in the threshold for ciliobrevin inhibition between the dynein activities that form principal and reverse bends, which disrupts the mechanisms required to maintain phase asymmetry, thereby inducing "phase asymmetry" in flagellar beating.

Heterogeneity of Dyneins

In mussel gill cilia, the dyneins on doublets 1–4 and 6–8 are expected to be active alternately during the effective and recovery stroke phases, respectively [Satir and Matsuoka, 1989]. This model of activity switching provides a good explanation of the planar beating during ciliary and flagellar motility based on axonemes with 9 + 2 circular symmetry in their cross-section. A *Chlamydomonas* mutant has been reported to have an asymmetric distribution of inner dynein

[King et al., 1994], thus there would be some functional heterogeneity in the dyneins among the peripheral doublet microtubules. From a structural viewpoint and based on the estimated hydrodynamic features of axonemes, it would also be reasonable to expect some functional differences in force generation and the rate of active sliding among the doublet sites in axonemes. Thus, the dynein arms that work alternately during the effective and recovery strokes in cilia, or that work during the principal and reverse bends in flagella, may exhibit some differences in terms of their mechanochemical properties. Our present study clearly indicates that ciliobrevin enhances the phase asymmetry of axonemal beats in sea urchin sperm flagella. Thus, we assume that a set of dynein arms that is responsible for reverse bends may be inhibited more severely compared with those responsible for principal bends. Hypothetically, the different sensitivities of dyneins to ciliobrevin inhibition may reflect the different structural properties of the ATP-binding sites in axonemal dyneins.

Our detection of beat asymmetry is also reminiscent of a description of the effects of Ni^{2+} in bull spermatozoa, where inhibition had selective effects on the dynein arms responsible for bending in one direction [Lindemann et al., 1995]. In the case of sea urchin spermatozoa, Nakano et al. [2003], reported that the microtubule sets that remained after disintegration were affected by calcium in the medium. In the present study, we occasionally observed that the motions of *H. depressus* spermatozoa were less sensitive to ciliobrevin in normal ASW, whereas they were blocked completely when the calcium concentration in BSA-ASW was reduced to 1/10th (data not shown). This may suggest that the different thresholds of dynein activity inhibition by ciliobrevin are also related to the site of calcium regulation in the dynein arms.

We hypothesize that there are differences in affinity for ciliobrevin and functional heterogeneity in the axonemal dyneins. Structural studies using cryo-electron tomography also suggest that there is structural heterogeneity in the axonemal components, including dynein ATPases and radial spoke heads [Bui et al., 2009; Maheshwari and Ishikawa, 2012; Lin et al., 2012; Heuser et al., 2012]. Although the structural heterogeneities described in these studies were focused in a narrow localized area of the axonemes and they might not correspond directly to the functional heterogeneity that we hypothesize here, this local structural heterogeneity could be enhanced by ciliobrevin and this may result in activity difference between the principal and reverse bends. Although we could not deny the possibility that ciliobrevin modifies the functions of other AAA-components in the axonemes [Bower et al., 2013], we expect this dynein heterogeneity among peripheral microtubules would be closely related to the beat-form regulation in cilia and flagella. In addition, as shown in the case of *Chlamydomonas* dynein arms [Yagi et al., 2009; Bui et al., 2012], our results also suggest that there would be longitudinal heterogeneity of dynein species in sea urchin sperm axonemes. Further experiments using ciliobrevin will help us to understand the structural and functional uniformity inside cilia and flagella.

Materials and Methods

Specimen Preparation

A. crassispina were collected at the Manazuru Peninsula in Kanagawa by Mr. Fumio Matsuzawa of Fumimaru, *P. depressus* were provided from the Misaki Marine Laboratory of University of Tokyo at Aburatsubo, Kanagawa. *H. pulcherrimus* were provided from Asamushi Marine Laboratory of Tohoku University at Aomori, or collected at Tateyama by the Marine Laboratory of Ochanomizu University at Chiba.

Sperm were collected by injecting 10^{-4} M carbamylcholine chloride (C-4382, Sigma) or 0.55 M KCl (163-03545, Wako) after removing the mouth, and maintained at 4 °C until use. Before the experiments, dry sperm were first diluted about 100 times with ASW (450 mM NaCl, 1 mM KCl, 10 mM $CaCl_2$, 2.5 mM $MgCl_2$, 2.8 mM $MgSO_4$, 10 mM Tris HCl, pH 8.2; Tris was obtained from Nakalai Tesque, Kyoto, Japan, and the other reagents were provided by Wako, Osaka, Japan) containing 0.1% BSA (BSA-ASW). A small aliquot of the suspension of intact spermatozoa was transferred into an experimental solution (see below), which was placed in a chamber made of a glass slide, two spacer strips (double-sided adhesive tape or dried manicure polymers), and a coverslip. We also observed the flagellar motion of spermatozoa after severing the flagellar tails. To make sperm tails short, the diluted sperm suspension (1 mL) was passed 10 times through a syringe (2.5 mL, Terumo) with a fine needle (27G, Terumo) before transferring to the experimental chamber.

Experimental Solution

Ciliobrevin (ciliobrevin A; HPI-4) was purchased from Sigma-Aldrich (St Louis, MO). Before use in the experiments, a 10 mM stock solution was prepared in dimethyl sulfoxide (Wako) and stored at −20 °C. The working solutions of ciliobrevin (0–100 μM) were prepared by diluting the stock solution with BSA-ASW and they were used within 1 day.

Measurement of the Beat Frequency

The frequency of flagellar beating was determined using a dark-field microscope (Olympus CX41; 40× Plan CN objective lens) equipped with stroboscopic illumination [modified from Baba and Mogami, 1987]. For flagellar beating faster than 10 Hz, the mean frequency was determined from the synchronized frequency of the strobe for at least 30 different spermatozoa in each experimental condition. For a beat frequency less than 10 Hz, the frequency

was determined by measuring the period of 10 beats manually using a stopwatch. For spermatozoa with severed short flagella, we determined the beat frequency using high speed video recordings, as described below.

High Speed Video Recording and Analysis of Sperm Motility

Images of motile spermatozoa were observed under a phase-contrast microscope (40× UPlan FlNH, NA = 0.75, IX2-LWUCD condenser on Olympus IX-70 inverted microscope) and recorded at 200 fps with a high speed camera (HAS-220, Ditect, Tokyo) driven by control software (V202_64) on a HP ProBook 4430s (64 bit, Windows 7). When we observed the swimming paths of spermatozoa (e.g., Fig. 1), spermatozoa images were recorded at a lower magnification (20× UPlan FlNH, NA = 0.50). To investigate the recovery of sperm motility after inhibition, we perfused the experimental chamber with a sufficient amount (volume, >10 times) of BSA-ASW without ciliobrevin.

The flagellar beat waveforms were analyzed using motion analysis software [Bohboh ver. 4.33; BohbohSoft, Tokyo, Japan; Ohmuro et al., 2004]. First, using an automatic tracking function of the motion analyzer, the *XY*-coordinates along the center line of a flagellar shaft were obtained for each spermatozoa image (total 100 frames for 0.5 s). The center line coordinates of flagella were determined as centroids based on a series of 1 μm segments placed along a sperm tail, which we used to calculate the waveform parameters, such as the curvatures and shear angles for each corresponding flagellar segment. Based on the microtubule sliding model for axonemal bending without twisting, we assumed that the shear angles and curvatures we obtained corresponded to the mean magnitudes of microtubule displacements and the differential value per unit flagellar length for each given flagellar segment. By fitting the time course of the shear-angle changes to a sinusoidal curve, we obtained a further parameter: the asymmetry index, which represented the phase asymmetry of flagellar beating. To calculate the asymmetry index, we used CUT (ver. 8.1, Evergreen Soft, Tokyo) and Bohboh_L (ver. 1.46, BohbohSoft). Depending on the beat frequency of the sperm flagella, some of the movie images recorded at 200 fps were reduced to 20 fps but the same number of frames was used in the motion analysis (in this case, 100 frames for 5 s).

Demembranation of Spermatozoa

Although ciliobrevin is a small molecule and it was expected to be fully membrane permeable, we also determined the effects after removing the flagellar membrane from the spermatozoa. To achieve demembranation, we followed the original method for Triton extraction described by Gibbons and Gibbons [1972] after minor modifications. Briefly, a portion of sperm (1 μL) was mixed with 5 μL ASW on ice and kept for 10 min. Next, 100 μL of demembranation solution (200 mM CH_3COOK, 2 mM $MgSO_4$, 1 mM EGTA, 0.1 mM EDTA, 0.04% Triton-X100, 1 mM DTT, 10 mM Tris HCl, pH 8.2) was added to the suspension of live spermatozoa and mixed. After keeping on ice for 40 s, 1 mL of reactivation solution without ATP (200 mM CH_3COOK, 2 mM $MgSO_4$, 1 mM EGTA, 0.1 mM EDTA, 0.1% PEG, 1 mM DTT, 0.1% BSA, 10 mM Tris HCl, pH 8.2) was added to end the Triton extraction. A small aliquot of the demembranated sperm was transferred to a solution containing 200 μM ATP plus 0, 50, or 100 μM ciliobrevin and placed on a slide glass to observe the flagellar motility, as described for live spermatozoa without demembranation.

Sliding Disintegration Experiments

For sliding disintegration experiments, demembranated sea urchin sperm was first prepared as mentioned above. The demembranated sperm (before ATP addition) was then passed through fine needles (27G, Terumo) for two to three times to make axonemal fragments. The resultant suspension was transferred into a chamber which was made of a glass slide and a cover slip separated with spacer strips (double-sided adhesive tape). Sliding disintegration was observed under a dark-field microscope (LUCPlanFLN 40x with U-DCW, Olympus IX71). To see the ciliobrevin effects, reactivating solution containing 100 μM ciliobrevin was first perfused and stayed for 1.5 to 15 min. Similarly, for the control experiment, reactivating solution without ciliobrevin was perfused and incubated for 10 min. Magnified images of axonemes before disintegration was recorded using a CCD camera (10 fps, EM-CCD (ImagEM) C9100-13, Hamamatsu-Photonics). After starting image recording, a buffer solution containing 2 μg/mL trypsin (T-8642, Sigma) plus 200 μM ATP was perfused into the chamber. Sliding disintegration event was usually observed in 15 to 60 s after starting the perfusion of trypsin-ATP solution.

Recorded movie images (saved as sequential tiff files) were analyzed using Image-J (ver.1.45s.). To determine the percentage of sliding disintegration, the Image-J option of image subtractions were used. The velocity of sliding was determined from the kymograph displays of disintegration axonemes showing linear microtubule sliding.

Acknowledgments

The authors thank those who provided sea urchins for their study; Mr. Fumio Matsuzawa of Fumimaru, Misaki Marine Laboratory of University of Tokyo, Asamushi Marine Laboratory of Tohoku University, and Tateyama Marine Laboratory of Ochanomizu University. The authors also thank Dr. Yoshihiro Mogami of Ochanomizu University for helpful discussions.

References

Baba SA, Mogami Y. 1987. Device for controlled intensification of the light output of xenon flash tubes. Rev Sci Instrum 58:1312.

Bower R, Tritschler D, Vanderwaal K, Perrone CA, Mueller J, Fox L, Sale WS, Porter ME. 2013. The N-DRC forms a conserved biochemical complex that maintains outer doublet alignment and limits microtubule sliding in motile axonemes Mol Biol Cell 15;24(8): 1134–1152.

Brokaw CJ, Kamiya R. 1987. Bending patterns of Chlamydomonas flagella: IV. Mutants with defects in inner and outer dynein arms indicate differences in dynein arm function. Cell Motil Cytoskeleton 8:68–75.

Bui KH, Sakakibara H, Movassagh T, Oiwa K, Ishikawa T. 2009. Asymmetry of inner dynein arms and inter-doublet links in Chlamydomonas flagella. J Cell Biol. 10;186(3):437–446.

Bui KH, Yagi T, Yamamoto R, Kamiya R, Ishikawa T. 2012. Polarity and asymmetry in the arrangement of dynein and related structures in the Chlamydomonas axoneme. J Cell Biol 198:913–925.

Firestone AJ, Weinger JS, Maldonado M, Barlan K, Langston LD, O'Donnell M, Gelfand VI, Kapoor TM, Chen JK. 2012. Small-molecule inhibitors of the AAA+ ATPase motor cytoplasmic dynein. Nature 484:125–129.

Gibbons BH. 1980. Intermittent swimming in live sea urchin sperm. J Cell Biol 84:1–12.

Gibbons BH, Gibbons IR. 1972. Flagellar movement and adenosine triphosphatase activity in sea urchin sperm extracted with triton X-100. J Cell Biol 541:75–97.

Heuser T, Barber CF, Lin J, Krell J, Rebesco M, Porter ME, Nicastro D. 2012. Cryoelectron tomography reveals doublet-specific structures and unique interactions in the I1 dynein. Proc Natl Acad Sci USA 2012;109(30):E2067–E2076.

Hiramoto Y, Baba SA. 1978. A quantitative analysis of flagellar movement in echinoderm spermatozoa. J Exp Biol 76:85–104.

King SM. 2012. Integrated control of axonemal dynein AAA(+) motors. J Struct Biol 179:222–228.

King SJ, Inwood WB, O'Toole ET, Power J, Dutcher SK. 1994. The bop2-1 mutation reveals radial asymmetry in the inner dynein arm region of chlamydomonas reinhardtii. Cell Biol 126:1255–1266.

Lin J, Heuser T, Carbajal-González BI, Song K, Nicastro D. 2012. The structural heterogeneity of radial spokes in cilia and flagella is conserved. Cytoskeleton (Hoboken) 69:88–100.

Lindemann CB, Walker JM, Kanous KS. 1995. Ni^{2+} inhibition induces asymmetry in axonemal functioning and bend initiation of bull sperm. Cell Motil Cytoskeleton 30:8–16.

Maheshwari A, Ishikawa T. 2012. Heterogeneity of dynein structure implies coordinated suppression of dynein motor activity in the axoneme. J Struct Biol 179:235–241.

Mocz G, Gibbons IR. 2001. Model for the motor component of dynein heavy chain based on homology to the AAA family of oligomeric ATPases. Structure 9:93–103.

Nakano I, Kobayashi T, Yoshimura M, Shingyoji C. 2003. Central-pair-linked regulation of microtubule sliding by calcium in flagellar axonemes. J Cell Sci 116:1627–1636.

Ohmuro J, Mogami Y, Baba SA. 2004. Progression of flagellar stages during artificially delayed motility initiation in sea urchin sperm. Zoolog Sci 21:1099–1108.

Satir P, Matsuoka T. 1989. Splitting the ciliary axoneme: implications for a "switch-point" model of dynein arm activity in ciliary motion. Cell Motil Cytoskeleton 14:345–358.

Wada Y, Mogami Y, Baba SA. 1997. Modification of ciliary beating in sea urchin larvae induced by neurotransmitters: beat-plane rotation and control of frequency fluctuation. J Exp Biol 200: 9–18.

Yagi T, Uematsu K, Liu Z, Kamiya R. 2009. Identification of dyneins that localize exclusively to the proximal portion of chlamydomonas flagella. J Cell Sci. 122(Pt 9):1306–1314.